



**HAL**  
open science

# Ultrafast non-thermal laser excitation of gigahertz longitudinal and shear acoustic waves in spin-crossover molecular crystals [Fe(PM-AzA)(2)(NCS)(2)]

T. Parpiiev, M. Servol, Maciej Lorenc, Ievgeniia F Chaban, R. Lefort, Eric Collet, H. Cailleau, P. Ruello, Nathalie Daro, Guillaume Chastanet, et al.

## ► To cite this version:

T. Parpiiev, M. Servol, Maciej Lorenc, Ievgeniia F Chaban, R. Lefort, et al.. Ultrafast non-thermal laser excitation of gigahertz longitudinal and shear acoustic waves in spin-crossover molecular crystals [Fe(PM-AzA)(2)(NCS)(2)]. Applied Physics Letters, 2017, 111 (17), 179901 (2 p.). 10.1063/1.5009657 . hal-01681154

**HAL Id: hal-01681154**


**<https://univ-rennes.hal.science/hal-01681154v1>**

Submitted on 23 Jan 2018

**HAL** is a multi-disciplinary open access archive for the deposit and dissemination of scientific research documents, whether they are published or not. The documents may come from teaching and research institutions in France or abroad, or from public or private research centers.

L'archive ouverte pluridisciplinaire **HAL**, est destinée au dépôt et à la diffusion de documents scientifiques de niveau recherche, publiés ou non, émanant des établissements d'enseignement et de recherche français ou étrangers, des laboratoires publics ou privés.

## AUTHOR QUERY FORM

	<b>Journal:</b> Appl. Phys. Lett.	Please provide your responses and any corrections by annotating this PDF and uploading it according to the instructions provided in the proof notification email.
	<b>Article Number:</b> 032741APL	

Dear Author,

Below are the queries associated with your article; please answer all of these queries before sending the proof back to AIP.

**Article checklist:** In order to ensure greater accuracy, please check the following and make all necessary corrections before returning your proof.

1. Is the title of your article accurate and spelled correctly?
2. Please check affiliations including spelling, completeness, and correct linking to authors.
3. Did you remember to include acknowledgment of funding, if required, and is it accurate?

Location in article	Query / Remark: click on the Q link to navigate to the appropriate spot in the proof. There, insert your comments as a PDF annotation.
<a href="#">AQ1</a>	Please check that the author names are in the proper order and spelled correctly. Also, please ensure that each author's given and surnames have been correctly identified (given names are highlighted in red and surnames appear in blue).
<a href="#">AQ2</a>	Please provide country and date of patent application.
<a href="#">AQ3</a>	Please verify the change in volume number in Ref. 3.
<a href="#">AQ4</a>	Please check the figure 2, and provide the revised figure file if necessary.

Thank you for your assistance.

# 1 Ultrafast non-thermal laser excitation of gigahertz longitudinal and shear 2 acoustic waves in spin-crossover molecular crystals [ $Fe(PM-AzA)_2(NCS)_2$ ]

3 T. Parpiiev,<sup>1</sup> M. Servol,<sup>2</sup> M. Lorenc,<sup>2,a)</sup> I. Chaban,<sup>1</sup> R. Lefort,<sup>2</sup> E. Collet,<sup>2</sup> H. Cailleau,<sup>2</sup>  
4 P. Ruello,<sup>1</sup> N. Daro,<sup>3</sup> G. Chastanet,<sup>3</sup> and T. Pezeril<sup>1,b)</sup>

5 <sup>1</sup>Institut Molécules et Matériaux du Mans, UMR CNRS 6283, Université du Maine, 72085 Le Mans, France

6 <sup>2</sup>Institut de Physique de Rennes, UMR CNRS 6251, Université de Rennes 1, 35042 Rennes, France

7 <sup>3</sup>Institut de Chimie de la Matière Condensée de Bordeaux, UPR CNRS 9048, Université de Bordeaux,  
8 33608 Pessac, France

9 (Received 17 July 2017; accepted 26 September 2017; published online xx xx xxxx)

10 We report GHz longitudinal as well as shear acoustic phonon photoexcitation and photodetection  
11 using femtosecond laser pulses in a spin-crossover molecular crystal. From our experimental obser-  
12 vation of time domain Brillouin scattering triggered by the photoexcitation of acoustic waves  
13 across the low-spin (LS) to high-spin (HS) thermal crossover, we reveal a link between the molecu-  
14 lar spin state and photoexcitation of coherent GHz acoustic phonons. In particular, we experimen-  
15 tally evidence a non-thermal pathway for the laser excitation of GHz phonons. We also provide  
16 experimental insights into the optical and mechanical parameters evolving across the LS/HS spin  
17 crossover temperature range. *Published by AIP Publishing.* <https://doi.org/10.1063/1.4996538>

18 Understanding how ultrafast photoinduced molecular  
19 switching in crystals couples to the lattice in optical materi-  
20 als is one of the key challenges in the fields of ultrafast  
21 photo-induced phase transitions or transformations and ultra-  
22 fast acoustics. Systems like spin-crossover compounds  
23 exhibit, with temperature or pressure, change of the molecu-  
24 lar spin state in the central  $d^4$ - $d^7$  transition metals of the  
25 complex. They are promising candidates for diverse applica-  
26 tions including miniature temperature sensors, displays, data  
27 storage, and photonic devices.<sup>1,2</sup> Moreover, they can be fab-  
28 ricated in a variety of forms (bulk, powders, matrices, and  
29 films) and down sizable to nanoparticles.<sup>2</sup> The possibility to  
30 trigger their properties by light,<sup>3</sup> especially in an ultrafast  
31 fashion, offers further prospects in future applications as  
32 optically controlled switching devices.<sup>2,4</sup> While such com-  
33 pounds have already been widely studied,<sup>5-8</sup> there is a short-  
34 age of information about the interplay between the change of  
35 the molecular spin state, the change of the unit cell volume  
36 (5% change), and the covalent bonding (10% change). From  
37 this standpoint, the study of crystal deformations that trigger  
38 excitation of coherent acoustic phonons clearly deserves fur-  
39 ther experimental investigations. Until now,<sup>9</sup> in the field of  
40 photo-induced phase transitions or transformations in molecu-  
41 lar crystals, the role of coherent optical phonons has been  
42 long under scrutiny because of the central role of optical  
43 mode softening, whereas that of coherent acoustic phonons  
44 and lattice deformations has not benefited from the same  
45 surge of effort. It is of paramount importance from the  
46 fundamental standpoint, as well as for the control of non-  
47 volatile information and energy storage, to further explore  
48 the pathways whereby acoustic phonons lead to non-volatile  
49 photo-induced states.

50 In the following, we describe our experimental results  
51 dealing with the photoexcitation of coherent acoustic phonons  
52 in a spin-crossover crystal, performed at different temperatures

53 around the spin crossover temperature  $T_{1/2}$ . The possibility of  
54 exciting with light pulse coherent acoustic phonons in a vari-  
55 ety of materials is well known;<sup>10,11</sup> however, unlike the longi-  
56 tudinal acoustic phonons, the shear acoustic phonons are  
57 difficult to photo-excite.<sup>12,13</sup> Our results highlight peculiar and  
58 efficient mechanisms for the photoexcitation of shear acoustic  
59 phonons and shed light on the interplay between molecular  
60 and elastic parameters in a spin-crossover compound.

61 In the present experiments sketched in Fig. 1(a),  
62 spin-crossover molecular crystals [ $Fe(PM-AzA)_2(NCS)_2$ ],  
63 schematically represented in the inset of Fig. 1(b), were  
64 investigated. These molecular crystals belong to the mono-  
65 clinic space group  $P2_1/c$  with one molecule as the asymmet-  
66 ric unit. In agreement with Refs. 5 and 7, the smooth thermal  
67 spin-crossover of these crystals with a spin crossover around  
68  $T_{1/2} \sim 180$  K can be monitored experimentally from the mea-  
69 surement of the magnetic susceptibility  $\chi_M$  and the product  
70  $\chi_M T$ , as indicated in Fig. 1(b). The experiments were per-  
71 formed on a parallelepipedic  $4 \times 1 \times 1$  mm<sup>3</sup> single crystal,  
72 with smooth, black color surfaces.<sup>7</sup> Due to large optical  
73 absorption by the crystal, front side pump-probe transient  
74 reflectivity measurements were performed, see Fig. 1(a). The  
75 pump and probe beams originate from a femtosecond Ti-  
76 Sapphire Coherent RegA 9000 regenerative amplifier operat-  
77 ing at a central wavelength of 800 nm and delivering 160 fs  
78 pulses at a repetition rate of 250 kHz. The 400 nm pump  
79 pulses of about 40 nJ energy per pulse were focused on the  
80 (110) surface of the crystal with a gaussian spatial profile of  
81 FWHM  $\sim 100$   $\mu$ m. The time delayed 800 nm probe of tenfold  
82 weaker energy per pulse, vertically polarized, was tightly  
83 focused at 30° oblique incidence on the (110) surface normal  
84 to the crystal and spatially overlapped with the pump spot.  
85 The reflected probe beam was directed to a photodiode cou-  
86 pled to a lock-in amplifier operating at 50 kHz of the pump  
87 laser modulation frequency, to measure transient differential  
88 reflectivity  $\Delta R(t)$  as a function of time delay between pump  
89 and probe beams. Upon transient absorption of the 400 nm  
90 pump pulse over the optical skin depth of the crystal, the light

a)Electronic mail: maciej.lorenc@univ-rennes1.fr

b)Electronic mail: thomas.pezeril@univ-lemans.fr

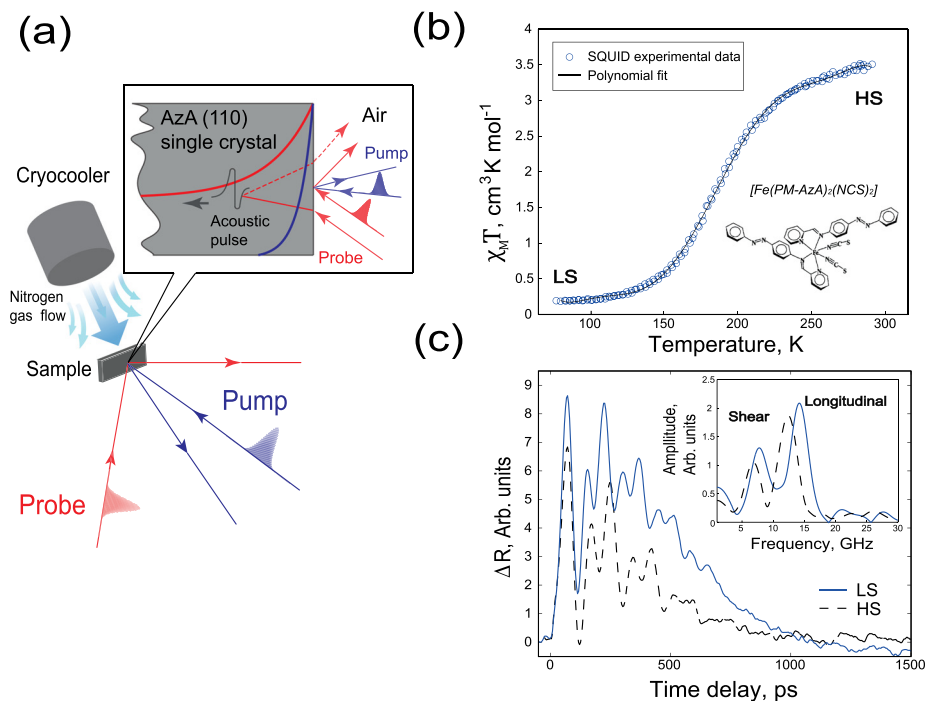


FIG. 1. (a) Sketch of the experimental setup. A laser pump pulse photoexcites the molecular crystal sample under continuous nitrogen flow for temperature control. The propagation of the photoexcited acoustic pulse is detected by a time-delayed optical probe pulse vertically polarized. (b) Schematic representation of the spin-crossover compound<sup>5</sup> and its magnetic susceptibility recorded across the smooth thermal spin-crossover temperature  $T_{1/2}$ . (c) Transient reflectivity signals recorded in the LS and HS states. The frequency spectrum of the LS and HS Brillouin oscillations shown in the inset gathers crucial information on the photoexcitation of both longitudinal and shear acoustic phonons.

91 energy is partially converted into mechanical energy that  
 92 drives the excitation of acoustic pulses propagating away  
 93 from the free surface. In the present situation, the crystal is  
 94 about five times less absorptive at 800 nm than at 400 nm,  
 95 see Fig. S1 in the [supplementary material](#), such that it can  
 96 be considered as semi-transparent at 800 nm and opaque at  
 97 400 nm. As a consequence, the pump light is locally absorbed  
 98 at the free surface where it launches a propagating acoustic  
 99 strain that backscatters the probe light from within the semi-  
 100 transparent medium and leads to the occurrence of time  
 101 domain Brillouin scattering oscillations, see Fig. 1(c). As in  
 102 any Brillouin scattering process, the frequency  $\nu$  of these  
 103 oscillations is related to the ultrasound velocity  $v$  of the crystal,  
 104 to the probe wavelength  $\lambda$ , to the refractive index  $n$  of the  
 105 medium, and to the back-scattering angle  $\theta$  through

$$\nu = 2 n v \cos \theta / \lambda. \quad (1)$$

106 The light activation of both longitudinal and shear acoustic  
 107 polarizations, of different ultrasonic speeds  $v$ , leads to two  
 108 distinct Brillouin frequencies. Figure 1(c) shows an example  
 109 of such time domain Brillouin scattering light modulation  
 110 where unambiguous periodic features at about 6 GHz and  
 111 12 GHz, see inset, are evidenced right after pump excitation  
 112 at zero time delay. The shear acoustic nature of the 6 GHz  
 113 frequency has been further experimentally confirmed from  
 114 depolarized Brillouin scattering measurements, see Fig. S2  
 115 in the [supplementary material](#), which enhances the optical  
 116 detection of shear acoustic waves.<sup>13</sup>

117 The experiments have been conducted at different tem-  
 118 peratures ranging from 100 K, where almost 100% of mole-  
 119 cules are in the low spin state, up to 300 K, where almost  
 120 100% of the molecules are in the high-spin state. Temperature  
 121 steps of 10 K were performed with a continuous nitrogen  
 122 flow. For each recorded time domain Brillouin scattering sig-  
 123 nal in the 100–300 K temperature range, we have numerically  
 124 fitted the experimental data with a damped sinusoidal function

in the form  $\sim A \exp(-t/\tau) \sin(2\pi\nu t + \phi)$ , to retrieve the fre- 125  
 quency  $\nu$ , the damping time  $\tau$ , the amplitude  $A$ , and the phase 126  
 $\phi$  of each longitudinal and shear acoustic mode. Based on the 127  
 results from ellipsometry available in the [supplementary mate- 128](#)  
 rial, which led to the observation of a slight variation of only a 129  
 few percent of the optical refractive index of the crystal at dif- 130  
 ferent temperatures, the huge 15% change in Brillouin fre- 131  
 quency in Fig. 2(a) is mainly due to a pronounced change in 132  
 both longitudinal and shear acoustic speeds with temperature. 133  
 According to Eq. (1) and the measured real part  $n_{\perp}$  of the 134  
 index of refraction at the probe wavelength for vertically polar- 135  
 ized light, see [supplementary material](#), we have computed the 136  
 change in Brillouin frequency to extract the variation in longi- 137  
 tudinal and shear acoustic speed with temperature. The results 138  
 displayed in Fig. 2(b) confirm the substantial change in acous- 139  
 tic speed, in the range of 10%, further emphasizing the giant 140  
 change in mechanical properties of the material across the spin 141  
 crossover temperature. This intrinsic softening of the material 142  
 at increasing temperature around  $T_{1/2}$  is coupled to a substan- 143  
 tial isostructural modification of the lattice parameters, mani- 144  
 fested in the change of the unit cell volume by as much as 145  
 $\sim 3\%$ .<sup>5,14</sup> 146

As a comparison with highly magnetostrictive ferromag- 147  
 netic compounds such as Terfenol<sup>15</sup> which is the foremost 148  
 highest magnetostrictive alloy with a change of the unit cell 149  
 volume by an amount of 0.1% upon modification of the mag- 150  
 netization vector, the change in  $[Fe(PM-AzA)_2(NCS)_2]$  lat- 151  
 tice parameters in the order of few % reveals the gigantic 152  
 spin state-lattice coupling in these molecular materials. The 153  
 pronounced molecular spin state-lattice coupling in such 154  
 compounds is bound to influence the generation of coherent 155  
 acoustic phonons. 156

The evolutions of the damping time coefficients with 157  
 temperature displayed in Fig. 2(c) are linked to the imagi- 158  
 nary part of the refractive index  $k_{\perp}$  at the probe wavelength 159  
 and to the intrinsic acoustic attenuation. From the measured 160  
 $k_{\perp}$  at the probe wavelength, we have processed the measured 161



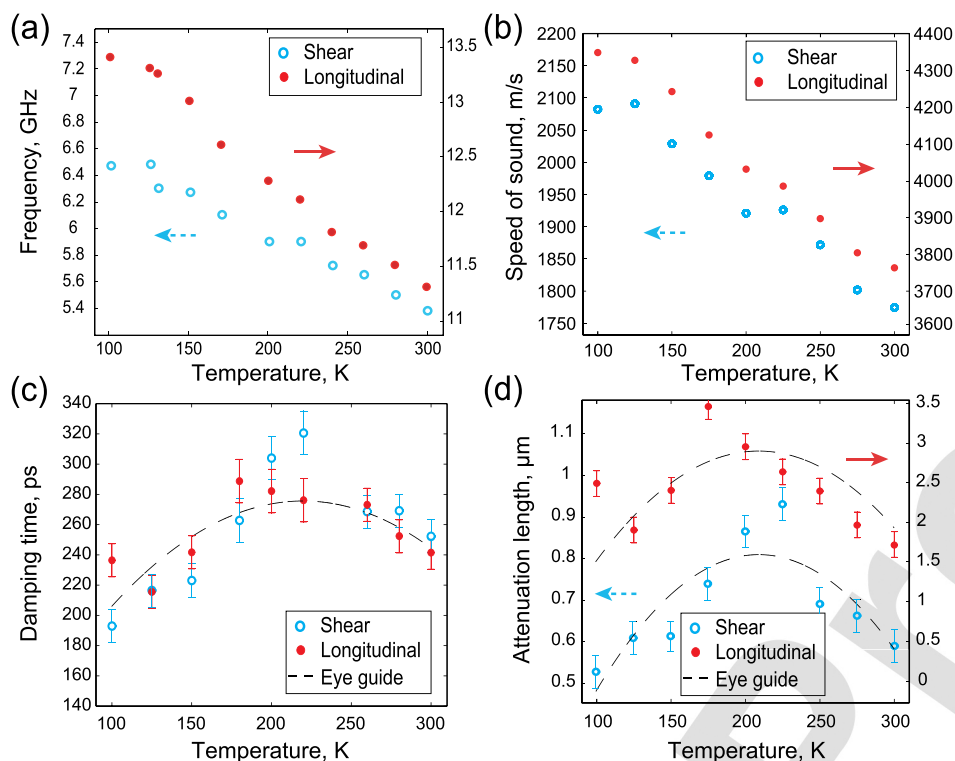


FIG. 2. From the time domain Brillouin scattering experimental data obtained for vertically polarized pump and probe beams at different temperatures, we have extracted the frequency (a) and the damping coefficient (c) of the measured Brillouin oscillations. In a second step, the temperature evolution of the index of refraction in the [supplementary material](#) led to the calculated acoustic speed (b) and acoustic attenuation length (d) of the longitudinal and shear acoustic modes across  $T_{1/2}$ . The eye guides are 2nd order polynomial fit of the extracted coefficients and the error bars are estimated from our experimental uncertainties.

AQ4

162 damping of the Brillouin oscillations  $\tau$ , in order to extract  
 163 the acoustic attenuation length  $\Gamma$  straightforwardly from  
 164  $\Gamma = v\tau - \zeta$ , where  $v$  is the longitudinal or shear acoustic speed  
 165 and  $\zeta = 4\pi k_{\perp}/\lambda$  is the optical penetration depth. Note that  
 166 the deconvolution of the acoustic damping in the measured  
 167 signals is not as straightforward in classical Brillouin spectroscopy  
 168 which sometimes requires complicated analyses  
 169 of the Brillouin linewidth of the peaks in the frequency  
 170 domain.<sup>16</sup> The result of the calculation of the acoustic attenuation  
 171 length for both acoustic modes, longitudinal and shear,  
 172 is displayed in Fig. 2(d). The remarkable maximum attenuation  
 173 length measured in Fig. 2(d) highlights a decrease in the  
 174 acoustic attenuation across the spin-phase crossover transition.  
 175 In the present case, the phenomenon is reversed from  
 176 the well-known structural  $\alpha$ -relaxation which has been evidenced  
 177 in glass forming liquids across the  $T_g$  glass transition  
 178 temperature.<sup>17</sup> The acoustic wave propagates on longer distances  
 179 at the spin-crossover temperature which indicates that  
 180 the structural modification of the lattice and the statistical  
 181 growth or disappearance of the LS/HS states do not perturb  
 182 the acoustic phonon propagation; on the contrary, the acoustic  
 183 phonon propagation is facilitated during the spin crossover  
 184 transition.

185 We can invoke several main mechanisms for the laser-driven  
 186 lattice motion in the present spin-crossover material:  
 187 the thermoelastic mechanism which is linked to the transient  
 188 thermal dilation of the lattice following the temperature rise  
 189 due to laser absorption and two non-thermal mechanisms,  
 190 namely, the molecular spin state-lattice coupling mechanism<sup>18</sup>  
 191 and the deformation potential mechanism.<sup>13</sup> The temperature  
 192 evolution of the Brillouin amplitudes and Brillouin phases  
 193 at two different pump polarizations [horizontal (H) and vertical (V)  
 194 polarizations] displayed in Fig. 3 gathers crucial information  
 195 on the photoacoustic excitation process.  
 196 The fact that the optical index of refraction does not vary

197 significantly with temperature warrants that the measured  
 198 Brillouin amplitude and phase are mainly sensitive to the  
 199 excitation mechanisms and not to the detection process  
 200 through a modification of the acousto-optic coefficients with  
 201 temperature. Since the measurement of the Brillouin amplitude  
 202 can suffer from experimental artifacts, such as beam  
 203 pointing stability during sample heating or cooling, we have  
 204 chosen to further process the longitudinal  $A_L$  and shear  $A_S$   
 205 Brillouin amplitudes data by taking the ratio of both amplitudes,  
 206 defined as  $A_L/A_S$ , not biased by optical artifacts. This  
 207 simple procedure highlights a discrepancy shown in Fig. 3(a)  
 208 that cannot be assigned to the thermoelastic mechanism.  
 209 In fact, as indicated by the difference in optical absorption  
 210 coefficients  $k_{\perp}$  and  $k_{\parallel}$  at the pump wavelength, see [supplementary material](#),  
 211 the laser induced temperature rise in such anisotropic crystals  
 212 depends on the pump polarization.  
 213 However, taking the ratio of amplitudes of both modes is a  
 214 proper way to conveniently remove the temperature rise  
 215 contribution in the thermoelastic process of acoustic excitation,  
 216 similar for longitudinal and shear acoustic modes. Therefore,  
 217 the gap between the amplitude ratio in Fig. 3(a) with H or V  
 218 polarizations is assigned to a non-thermal mechanism, either  
 219 molecular spin state-lattice coupling or deformation potential  
 220 mechanism. One possible explanation of the observed amplitude  
 221 jump would be the anisotropy in the deformation potential  
 222 mechanism. The latter should be considered as tensorial  
 223 in such crystals with different diagonal and non-diagonal  
 224 coefficients referring to preferential electronic excitations  
 225 of the ligands by horizontally or vertically polarized pump  
 226 pulses, with some similarities with Ref. 19 that demonstrates  
 227 the wide range of electronic excitations of organic molecules  
 228 that can drive coherent lattice phonon excitation. In addition  
 229 to the electron deformation potential mechanism, we cannot  
 230 neglect the molecular spin state-lattice coupling anisotropy,  
 231 thus revealing pump laser polarization dependence.

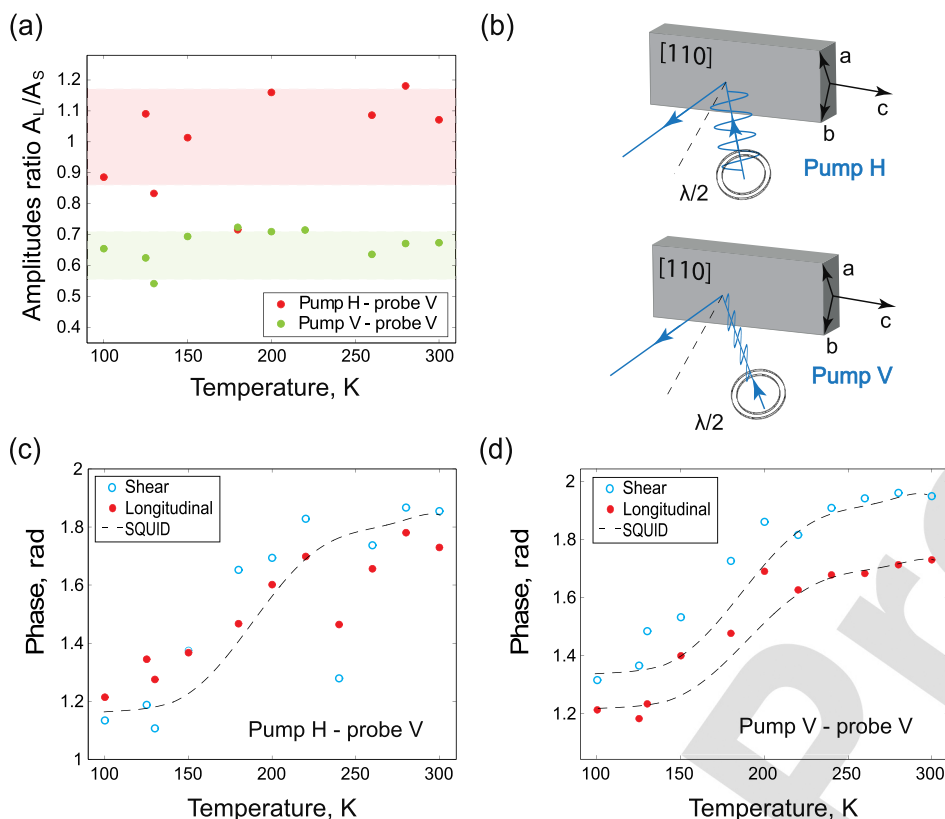


FIG. 3. (a) Ratio between the longitudinal and shear Brillouin amplitudes for different pump polarizations. Red dots correspond to the horizontally polarized pump and green to the vertically polarized pump, as sketched in (b). Extracted time domain Brillouin phase for horizontally (c) and vertically (d) polarized pump beams of both longitudinal and shear acoustic modes in the compound at different crystal temperatures. The SQUID curve matches the Brillouin phase evolution across  $T_{1/2}$ .

Another striking feature suggesting coexistence of photoacoustic mechanisms is revealed by the Brillouin phase change in Figs. 3(c) and 3(d) with H or V pump polarizations. Once again, if we assume that the slight change with temperature of the optical index of refraction is irrelevant for the interpretation of our experimental observations, the substantial phase jump in the range of 0.6 radians of both longitudinal and shear Brillouin signals across the spin-crossover transition highlights a profound change in the laser-matter mechanism for acoustic phonons excitation. Based on Ref. 20, we can interpret this phase change, which correlates with the magnetic susceptibility of Fig. 1(b), as a change in the acoustic excitation process through the contribution of the spin state-lattice mechanism that vanishes once the compound reaches 100% HS spin. However, the photoinduced spin state-lattice coupling is maybe not the most efficient at this pump wavelength. Therefore, we cannot rule out the deformation potential mechanism as relevant in the process of laser excitation of coherent acoustic phonons in the present spin crossover material. The observation of the phase jump of about 0.2 radians in Fig. 3(d) between longitudinal and shear excitation points to a non-thermal mechanism of acoustic excitation sensitive to the pump polarization, as in Fig. 3(a). As a matter of fact, based on the results presented in Fig. 3, we can conclude that two non-thermal mechanisms are triggered in these molecular crystals, each one having different efficiency (amplitudes) and characteristic times (phases).

In summary, we have performed ultrafast time-domain Brillouin scattering experiments to study non equilibrium dynamics following femtosecond photoexcitation of spin-crossover molecular crystals  $[Fe(PM-AzA)_2(NCS)_2]$ . We have presented results for coherent GHz acoustic phonons photo-generation and photodetection in a spin-crossover material

across the spin-crossover temperature range. Through time domain Brillouin scattering, we evidence non-thermal excitation of acoustic phonons which are of spin state-lattice coupling and/or deformation potential origin. Experimentally revealed on the sub-nanosecond time-scale, remarkable sensitivity of Brillouin frequencies to the spin state of a molecular material opens advanced perspectives for probing macroscopically relevant processes during a phase transition. We envisage pump-pump-probe experiments, in which the molecular spin-state is photoexcited with wavelength tuned pump pulse, while the real-time coupling of thus generated spin-states to the lattice is followed by the second pump through time-resolved Brillouin scattering, such as this work. Furthermore, our results highlight the versatile and efficient generation of ultrashort shear acoustic phonons for future investigations of viscoelastic properties of materials such as liquids,<sup>21</sup> glasses,<sup>22,23</sup> mixed multiferroics, correlated electron systems, and magnetic materials. Ultimately, deeper knowledge of the spin state-elastic coupling in spin-crossover molecular crystals will be crucial for the design of multifunctional molecular devices.

See supplementary material for the temperature data of the real  $n$  and imaginary  $k$  refractive index of  $[Fe(PM-AzA)_2(NCS)_2]$  at 400 nm and 800 nm wavelengths, as for a comparison between transient reflectivity and depolarized Brillouin scattering.

The authors are thankful to Pr. Vitalyi Gusev for beneficial scientific discussions and guidance and to Lionel Guilmeau for technical support. The authors gratefully acknowledge Agence Nationale de la Recherche for financial support under grants ANR-16-CE30-0018, ANR-14-CE26-0008, and ANR-12-BS09-0031-01.

- 299 <sup>1</sup>J.-F. Létard, P. Guionneau, and L. Goux-Capes, *Top. Curr. Chem.* **235**, 321 (2004). 322
- 300 221 (2004). 322
- 301 <sup>2</sup>A. Bousseksou, G. Molnár, L. Salmona, and W. Nicolozzia, *Chem. Soc. 323*
- 302 *Rev.* **40**, 3313 (2011). 324
- 303 <sup>3</sup>A. Hauser, J. Jeftić, H. Romstedt, R. Hinek, and H. Spiering, *Coord. 325*
- AQ3 304 *Chem. Rev.* **190–192**, 471 (1999). 326
- AQ2 305 <sup>4</sup>J.-F. Létard and E. Freysz, patent WO2012010801 A1 (■ ■ 2012). 327
- 306 <sup>5</sup>P. Guionneau, J.-F. Létard, D. S. Yufit, D. Chasseau, G. Bravic, A. E. 328
- 307 Goeta, J. A. K. Howard, and O. Kahn, *J. Mater. Chem.* **9**, 985–994 (1999). 329
- 308 <sup>6</sup>A. Goujon, F. Varret, K. Boukheddaden, C. Chong, J. Jeftić, Y. Garcia, A. D. 330
- 309 Naik, J. C. Ameline, and E. Collet, *Inorg. Chim. Acta* **361**, 4055 (2008). 331
- 310 <sup>7</sup>A. Marino, M. Servol, R. Bertoni, M. Lorenc, C. Mauriac, J.-F. Létard, 332
- 311 and E. Collet, *Polyhedron* **66**, 123 (2013). 333
- 312 <sup>8</sup>Y. Jiang, L. Chung Liu, H. M. Muller-Werkmeister, C. Lu, D. Zhang, R. 334
- 313 L. Field, A. Sarracini, G. Moriena, E. Collet, and R. J. Dwayne Miller, 335
- 314 *Angew. Chem. Int. Ed.* **56**, 7130 (2017). 336
- 315 <sup>9</sup>R. Bertoni, M. Lorenc, H. Cailleau, A. Tissot, J. Laisney, M.-L. Boillot, L. 337
- 316 Stoleriu, A. Stancu, C. Enachescu, and E. Collet, *Nat. Mater.* **15**, 606 (2016). 338
- 317 <sup>10</sup>J.-F. Létard, J. A. Real, N. Moline, A. B. Gaspar, L. Capes, O. Cadot, and 339
- 318 O. Kahn, *J. Am. Chem. Soc.* **121**, 10630–10631 (1999). 340
- 319 <sup>11</sup>C. Thomsen, H. T. Grahn, H. J. Maris, and J. Tauc, *Phys. Rev. B* **34**, 4129 341
- 320 (1986). 342
- <sup>12</sup>T. Pezeril, P. Ruello, S. Gougeon, N. Chigarev, D. Mounier, J.-M. 321
- Breteau, P. Picart, and V. Gusev, *Phys. Rev. B* **75**, 174307 (2007). 322
- <sup>13</sup>T. Pezeril, *J. Opt. Laser Technol.* **83**, 177 (2016). 323
- <sup>14</sup>N. Klinduhov, D. Chernyshov, and K. Boukheddaden, *Phys. Rev. B* **81**, 324
- 094408 (2010). 325
- <sup>15</sup>O. Kovalenko, T. Pezeril, and V. Temnov, *Phys. Rev. Lett.* **110**, 266602 326
- (2013). 327
- <sup>16</sup>J. R. Sandercock, *Light Scattering in Solids III* (Springer Berlin 328
- Heidelberg, Berlin, 1982), pp. 173–206. 329
- <sup>17</sup>Y. Yang and K. A. Nelson, *J. Chem. Phys.* **103**, 7732 (1995). 330
- <sup>18</sup>C. Enachescu, L. Stoleriu, M. Nishino, S. Miyashita, A. Stancu, M. 331
- Lorenc, R. Bertoni, H. Cailleau, and E. Collet, *Phys. Rev. B* **95**, 224107 332
- (2017). 333
- <sup>19</sup>A. Rury, S. Sorenson, and J. Dawlaty, *J. Chem. Phys.* **144**, 104701 (2016). 334
- <sup>20</sup>G. Vaudel, T. Pezeril, A. Lomonosov, M. Lejman, P. Ruello, and V. E. 335
- Gusev, *Phys. Rev. B* **90**, 014302 (2014). 336
- <sup>21</sup>T. Pezeril, C. Klieber, S. Andrieu, and K. A. Nelson, *Phys. Rev. Lett.* **102**, 337
- 107402 (2009). 338
- <sup>22</sup>C. Klieber, T. Pezeril, S. Andrieu, and K. A. Nelson, *J. Appl. Phys.* **112**, 339
- 013502 (2012). 340
- <sup>23</sup>C. Klieber, T. Hecksher, T. Pezeril, D. Torchinsky, J. Dyre, and K. 341
- Nelson, *J. Chem. Phys.* **138**, 12A544 (2013). 342